Intermediate temperature solid oxide fuel cell electrolytes

Massimiliano Lo Faro, Daniela La Rosa, Vincenzo Antonucci AND Antonino Salvatore Aricó

Abstract | Solid Oxide Fuel Cells (SOFCs) have suitable perspectives to replace their classical counterparts for the distributed generation of electrical energy with small and medium power sources (50 kWel). The main advantages of SOFCs rely on the high conversion efficiency and low environmental impact. Practical SOFC operating temperatures between 600 °C and 800 °C are aimed to increase life-time and reduce costs. These can be achieved only by using electrolytes with proper ionic conductivity at intermediate temperatures. This review deals with a survey of the current research on advanced materials to be used as electrolyte for intermediate or low temperature solid oxide fuel cells. Specific properties such as reaction mechanism, chemical compatibility, effects of dopants, and conductivity are discussed.

1. Introduction

The current energy supply systems, which are mainly based on the combustion of fossil fuels, cause many environmental problems: air pollution, acid gas emissions, and the emission of greenhouse gases. At the same time supply of electricity and transport of goods/persons are the basis of modern life. These two sectors are strongly related to mass consumption of energy. The increasing energy demands and emerging energy crisis pose the question on how energy can be used in the earth more efficiently while keeping our environment clean. One of the most urgent problems in the 21st century will regard both conservation of energy resources and decrease of CO_2 emission. This problem can be translated in term of reduction of consumption of energy in developed countries and increase the use of advanced/efficient energy systems at a large scale level. These requirements can be summarized as "highly efficient technology in electricity generation and transportation".

Solid-state ionic devices, such as SOFCs are promising energy conversion and storage technologies that could solve some environmental issues, while simultaneously curbing the consumption of resources and providing employment opportunities. Solid oxide fuel cells (SOFC) are expected to play a major role in the stationary generation of energy as well as in transportation in the coming decades.

The solid oxide fuel cell is currently attracting tremendous interest because of its huge potential to enhance energy conversion efficiency, reliability and security, and reducing environmental impact. As well as, fuel flexibility is one of the significant advantages of solid oxide fuel cells (SOFCs) over other types of fuel cells The major drawback in commercializing SOFCs is concerning with high costs which result from the use of special high temperature ceramic materials.

One important aspect in the use of solid oxide fuel cells is the high operating temperature

CNR-ITAE Institute, Via Salita S. Lucia sopra Contesse 5 IT-98126 Messina, Italy
arico@itae.cnr.it

Keywords: Fuel cells, Solid Oxides, Ceramic electrolytes, Ceria, Protonic electrolytes, Anionic electrolytes, Power sources

Figure 1: A Solid Oxide Fuel Cell.

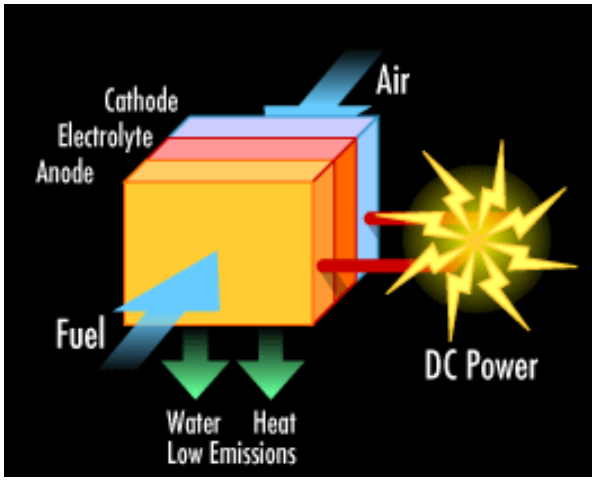

required to obtain optimal ionic conductivity using conventional electrolytes. Moreover, operating temperatures higher than 800 °C demand the use of expensive ceramic interconnectors based on lanthanum chromite, and at the same time, significantly reduce the lifetime of these devices. Practical operating temperatures between 600 °C and 800 °C can be achieved by using electrolytes that have high levels of conductivity at low temperatures. This review aims to provide an overview of present research in the field of electrolytes for IT-SOFCs.

The fundamental aspects of SOFC operation will be presented first; the challenges of the current research and an outline of the recent activities will be discussed. The emphasis is placed on the development of electrolytes that can work in the temperature range 400–750 °C as alternative to the classical yttria stabilized zirconia operating above 750 °C.

2. Principles of operation

A Solid Oxide Fuel Cell (SOFC) is an energy conversion device that produces electricity by electrochemically combining a fuel and an oxidant across an ionic conducting electrolyte, the principles of operation are illustrated in Fig. 1.

The dense electrolyte is sandwiched between two porous electrodes, the anode and the cathode (the anode/electrolyte/cathode sandwich is referred to as a single cell). Fuel is fed to the anode, it undergoes an oxidation reaction, and releases electrons to the external circuit. Oxidant is fed to the cathode, accepts electrons from the external circuit, and undergoes a reduction reaction. The electron flow in the external circuit from the anode to the cathode produces electricity.

Under operation, the SOFC can use either an oxygen ion-conducting electrolyte or a proton-conducting electrolyte. Most current research efforts have been focusing on the SOFC with the oxygen ion-conducting electrolyte (SOFC-O^{2-}) rather than with the proton-conducting electrolyte (SOFC-H^{+}).

The difference in ion activity on the two electrodes provides a driving force for motion of the ions in the electrolyte. In the case of SOFC-O^{2-}, oxide ions formed by dissociation of oxygen at the cathode under electron consumption migrate through the electrolyte to the anode where they react with the oxidation products to form water, heat, and CO_2; similarly it occurs in the case of SOFC-H^{+}, protons produced at the anode migrate through the electrolyte to the cathode where they react with oxygen and electrons forming water and heat.

The electrochemical reactions occur in the electrodes within a distance of less than 10–20 microns from the electrolyte surface[1,2]. This zone is referred to as the functional layer. The part of the electrode exceeding this thickness is primarily a current collector structure, which must be porous to allow gas access to the functional layer. The electrolyte has to be gas impermeable to avoid direct mixing and combustion of the gases. The electrolyte is ceramic, and the electrodes are also based on ceramic materials. Under cell operating conditions, the cell produces current as long as the reactants are provided to the electrodes. An open circuit voltage (OCV) of slightly larger than 1 volt is attained when

Figure 2: Fuel cell polarisation (voltage vs. current density) and power density curves[3].

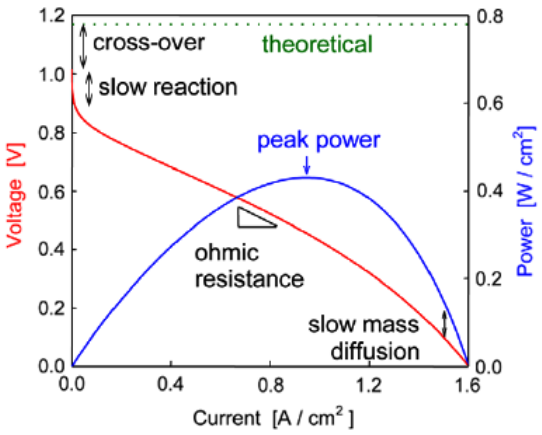

the cell is not loaded, and ionic transport number is close to 100%. The Nernst potential, E, gives the ideal open circuit cell potential. This potential sets the upper limit or maximum voltage achievable by a fuel cell.

Connected to an external load, the potential difference across the electrodes of a fuel cell drives the electrons through the external circuit. However, the detailed processes in the electrochemical system are quite complex in nature.

Even though many studies have been devoted to the charge transfer at the interfaces formed by the electrodes and solid electrolyte, it still remains one of the least understood aspects of electrochemistry.

The operation of the cell is associated with various irreversibilities and leads to various potential losses. In the case of electrodes, the total resistance comprises of the internal, contact, activation, and mass transport resistances. Internal resistance refers to the electron transport in the electrode and ionic transport in the electrolyte which are determined by the electronic and ionic conductivity respectively and the thickness of the electrode and electrolyte. Contact resistance refers to the poor contact between the electrode and the electrolyte structure. All resistive losses are functions of the local current density. The overpotential losses can be minimized by an appropriate choice of electrode material and the control of the micro-structural properties during the manufacturing process.

The performance measure of a SOFC is the voltage output as a function of electrical current density drawn in the external circuit, it represents a deviation from Nernst potential and is called polarisation curve.

As shown in Fig. 2, there are three types of polarisations and regions of operation wherein a particular loss mechanism is dominant relative to the other polarisations. At and near open circuit voltage (low current densities), activation polarisation is the dominant loss term; it is caused by slow reaction. At intermediate current densities, ohmic voltage decrease is the dominant loss mechanism. Ohmic losses obey Ohm's Law in terms of proportionally increasing as current increases. Ohmic losses are associated with the resistance (i.e. area-specific- resistance or ASR) mainly caused by the electrolyte and interfacial surfaces. At higher current demands, concentration polarisation is the dominant overpotential.

The measured voltage, E, can be written as

$$E = E_{\text{eq}} - E_L - \eta_{\text{act}} - \eta_{\text{ohm}} - \eta_{\text{diff}} \qquad (2.1)$$

where E_{eq} is the equilibrium (expected or Nernstian voltage), E_L is the loss in voltage due to leaks across the electrolyte, η_{act} is the activation overpotential due to slow electrode reactions; η_{ohm} is the overpotential due to ohmic resistances in the cell; and η_{diff} is the overpotential due to mass diffusion limitations.

The impact of all the terms of Eq. (2.1) is highlighted in Fig. 2.

The efficiency of fuel cells is much higher than those of combustion engines because they are not governed by the Carnot Cycle[4–6] because the energy conversion pathway does not proceed via thermal energy but directly from chemical into electrical energy. Thus, the chemical reaction is controlled in such a way that the electron exchange does not take place locally but via an external circuit. The fuel cell is therefore a part of the electrical circuit.

SOFC efficiency can be split into three terms: Thermodynamic Efficiency (intrinsic fuel

Figure 3: Comparison of specific electricity and heat generation in a SOFC[7].

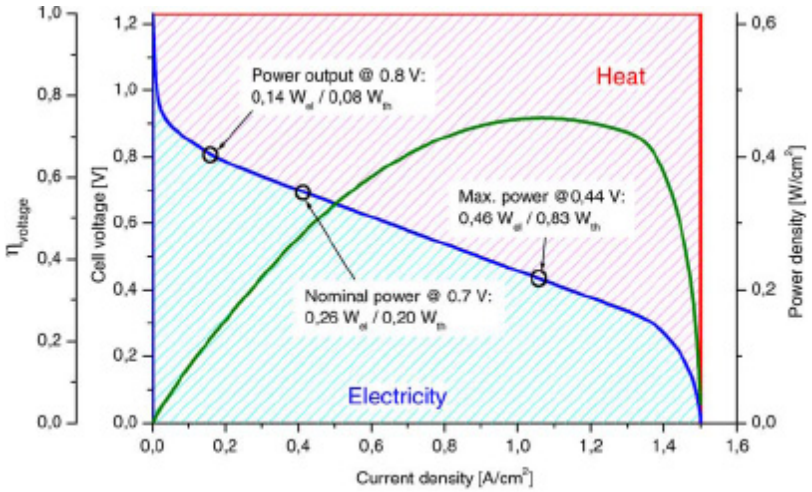

properties), Voltage Efficiency (ability to realise ideal voltage) and Current Efficiency (ability to utilise supplied fuel).

$$\mathcal{E}_{SOFC} = \mathcal{E}_T \times \mathcal{E}_V \times \mathcal{E}_I \tag{2.2}$$

The maximum thermodynamic efficiency, $\mathcal{E}_T$ is determined by the intrinsic fuel properties. It demonstrates the desirability of electrochemically oxidising a fuel and that some fuels can be more advantageously electrochemically oxidised than others. The voltage efficiency, $\mathcal{E}_V$, is related to the fact that the operating voltage of a cell is always less than the theoretical maximum. On the other hand, current efficiency, $\mathcal{E}_I$, is reduced if not all reactants are converted to reaction products, or if some electrons are involved in alternative reactions as in the case of corrosion or parasite current into the electrolyte.

SOFCs provide many advantages over traditional energy conversion systems including high efficiency (in the range 45–60%), reliability, modularity, and extremely low emissions of major local air pollutants (CO, NO_x, and unburned hydrocarbons). A SOFC converts the chemical energy of fuel directly into electrical energy. Thus, the usual losses involved in the conversion of fuel to heat, to mechanical energy, and then to electrical energy of conventional combustion systems are avoided. SOFCs can potentially be operated on a range of fuels, including pipeline natural gas and bio-mass, without a significant loss of efficiency or increase in system complexity and cost.

SOFC systems are presently rated at a cell voltage of 0.7 V/cell. While this is a reasonable approach for performance comparisons and exhibits a high electric power output (>50% of the maximum), there are also some disadvantages. As can be seen in Fig. 3, the electrical efficiency is restricted to 56% by the electricity/heat ratio of 1.3. The cell generates approximately 0.75 W heat/W electricity. Removal of the heat needs large amounts of air which affect stack, heat exchanger and blower design. However, this heat can be further converted in a combined heat and power (CHP) system with a significant increase of the overall efficiency.

A rise of the cell voltage for example to 0.8 V/cell implies an 80% increase in cell area and therefore stack size for the same electric output. However, the electricity/heat ratio increases from 1.3 at 0.7 V to 1.75 at 0.8 V. The cell efficiency is then raised to 64%. The resulting lower heat load reduces the size of peripherals like tubing, heat exchanger and blower, and also the power consumption of active cooling systems like blowers and pumps.

3. Electrolyte

The main purpose of an electrolyte is to conduct a specific ion between two electrodes in order to complete the overall electrochemical reaction. Without conduction of that specific ion, no appreciable current would be able to flow through the fuel cell and only potential would exist.

With the advancements in fabrication technology, the overall performance of SOFCs is eventually limited by the conductivity of the electrolyte materials. Ideally, an electrolyte is an ionic conductor and an electronic insulator. SOFC electrolytes work in the most stringent environment:

hydrogen or hydrocarbons on the anode side, oxygen on the cathode side, and also high temperatures.

Solid oxide fuel cells are based on the concept of an oxygen ion conducting electrolyte through which the oxide ions (O^{-2}) migrate from the air electrode (cathode) side to the fuel electrode (anode) side where they react with H_2 to form water and electricity. In the case where hydrocarbons serve as the fuel, an oxygen ion conductor offers, in principle, the prospect of direct electro-oxidation:

$$CH_4 + O^{2-} \rightarrow CO_2 + 2H_2O + 8e^- \qquad (3.1)$$

Generally, it is instead presumed that the high temperature of operation associated with oxygen ion conductors can be used to facilitate internal steam reforming:

$$CH_4 + H_2O \rightarrow CO + 3H_2 \qquad (3.2)$$

with CO and H_2 then used in the electro-oxidation reactions. Even in this more conservative scenario, oxygen-ion conducting electrolytes are preferred because CO can be electro-oxidized, rather than (particularly in the case of low temperature systems) poisoning the anode catalyst. Ceramic proton conductors may offer an interesting combination of benefits because of their ability to transport both protons and oxygen ions. It has been suggested[8] that water can diffuse across the electrolyte membrane, inducing steam reforming and even conversion of CO to CO_2 through the water-gas shift reaction:

$$CO + H_2O \rightarrow CO_2 + H_2 \qquad (3.3)$$

Hydrogen generated by reactions (3.2) and (3.3) is then electro-oxidised to form protons. In this case, hydrocarbons can be directly utilized and no water is produced at the anode, again avoiding dilution effects as fuel utilization increases (although CO2 dilution still occurs).

Fundamentally, for optimum cell performance, the electrolyte must be free of porosity so as not to allow gases to permeate from one side of the electrolyte to the other, it should be uniformly thin to minimize ohmic loss, and it should have high ion conductivity with transport number for ions close to unity and a transport number for electrons as close to zero as possible. At the end, electrolytes with these desired properties must be deposited as thin as possible in order to work with low ohmic loss.

The general criteria for the quality of a solid electrolyte material to be used in a SOFC are:

(a) Easy of fabrication into a mechanically strong dense membrane of small thickness and large area to minimize bulk resistance.
(b) An oxide-ion conductivity $\sigma_0 > 10^{-2}$ S cm^{-1} at the cell operating temperature.
(c) Excellent chemical and mechanical compatibility with electrodes to avoid formation of blocking interface phases and minimize interfacial resistances.
(d) A negligible electronic conductivity at cell operating temperature to retain a transport number close to 1.
(e) Compatibility of thermal-expansion coefficients between electrolyte, electrodes, interconnects, and seals from ambient temperature and cell operating temperature.
(f) Relatively low costs of material and fabrication.

3.1. *Oxygen ion conductors*

Most current research efforts have been focusing on the SOFC with the oxygen ion-conducting electrolyte (SOFC-O^{2-}).

In oxygen ion conductors, current flow occurs by the movement of oxide ions through the crystal lattice. This movement was shown to be dominated by oxygen ions vacancies over 100 years ago by Nernst[9], and is a result of thermally-activated hopping of the oxygen ions inside the crystalline lattice, with a superimposed drift in the direction of the electric field. The ionic conductivity is consequently strongly temperature dependent, but at high temperatures can approach values close to 1 S cm^{-1}, comparable to the levels of ionic conductivity found in liquid electrolytes. This is clearly a remarkable property of these solids and to understand its origins we must make several important observations. The first observation is that the crystal must contain unoccupied sites equivalent to those occupied by the lattice oxygen ions. Secondly, the energy involved in the process of migration from one site to the unoccupied equivalent site must be small, certainly less than about 1 eV.

Oxides with high ionic have open structure, such as fluorite and pyrochlore. Almost all SOFC systems currently being developed employ a stabilized zirconia (ZrO_2), especially yttria stabilized zirconia, because this material has an adequate level of oxide ionic conductivity and shows the desirable stability in both oxidizing and reducing environments, as well it is also abundant, relatively low in cost and is strong whilst being easy to fabricate.

In general, at room temperature, pure zirconia is monoclinic and undergoes a phase transition to a tetragonal structure above 1170 °C. In addition, above 2370 °C, zirconia can be transformed into cubic fluorite structure. The tetragonal-monoclinic transformation is associated with a large volume change (3–5%) (contraction on heating and

expansion on cooling). The cubic phase still exists up to the melting point at 2680 °C. However, the doping of certain aliovalent oxides stabilizes the cubic fluorite crystal structure of zirconia from room temperature to its melting point and simultaneously increases oxygen vacancy concentration. The oxygen vacancies for a typical trivalent dopant, M, can be written in the Kröger–Vink notati[10]:

$$M_2O_3 \xrightarrow[ZrO_2]{} 2M_{Zr} + 3O_O^x + V_O^{\bullet\bullet} \qquad (3.4)$$

with one oxygen vacancy created for every two M atoms incorporated.

From these reasons, the ionic conductivity can be enhanced, and the oxygen partial pressure range of ionic conduction can be extended, making stabilized zirconia suitable for use as an electrolyte in SOFCs. The most commonly dopants are CaO, MgO, Y_2O_3, Sc_2O_3, and certain rare earth oxides[11–20]. These oxides must have a relatively high solubility in zirconia and must be stable to form the fluorite structure. It is generally found that the ionic conductivity has a maximum near the minimum level of dopant oxide required to fully stabilize the fluorite-type phase[21–24]. The conductivity increases then decreases across the rare earth series from Yb to La. At higher dopant levels the ionic conductivity decreases, which is attributed to defect ordering, vacancy clustering or electrostatic interaction[25]. Although some other oxide dopants produce cubic stabilised zirconia with higher ionic conductivities than yttria stabilised zirconia, yttria is the most widely used dopant for reasons of cost, availability and stability in oxidising and reducing atmospheres, and its chemical inertness towards other components in the SOFC. There are a number of study that have shown how the conductivity of YSZ increases for yttria additions of up to about 8 mol. % and then decreases for higher yttria contents[11,12,26,27]. The decrease at higher dopant contents is due to association of point defects, which leads to a reduction in defect mobility and thus conductivity. Conventional zirconia based SOFCs generally require an operating temperature above 850 °C. The operating temperature is principally governed by the nature of the electrolyte, i.e. its ionic conductivity, and the thickness of the electrolyte layer. There are therefore two possible approaches to lowering the operating temperature. The first is to reduce the thickness of the YSZ electrolyte layer, whilst the second is to search for alternative electrolyte materials with higher oxygen ion conductivities. SOFCs currently being developed which do not rely on the solid electrolyte for structural support typically have an electrolyte layer around 30 μm thick. In such SOFCs the electrolyte must be supported on another substrate, which is in some cases the anode or the cathode. The search for, and study of, alternative solid electrolyte materials has been an active research area for many years. A promising, though less widely used, dopant for zirconia is scandia, which has a higher ionic conductivities, though it is also more expensive than YSZ. Appropriate scandium doping and microstructure optimisation for zirconia electrolytes[28] has resulted in oxygen conductivity as high as 0.15–0.20 S cm^{-1} at 1000 °C. The higher conductivity of ScSZ is attributed to the smaller mismatch in size between Zr^{4+} and Sc^{3+}, as compared to that between Zr^{4+} and Y^{3+}, leading to a smaller energy for defect association, which increases mobility and thus conductivity[27,29–31]. It is commonly accepted that this tendency increases with increasing difference between the host and dopant cation radii[23,32–35]. Similar phenomena explain the conductivity variations in numerous fluorite and pyrochlore systems.

Yamamoto and co-workers[15] have explained how during operation, aging of both YSZ and ScSZ can lead to decreases in conductivity. Nomura[27] has reported that the magnitude of the decrease in conductivity during aging is larger for YSZ than for ScSZ, such that, after 5000 h, the conductivity of ScSZ, which was initially about twice that of YSZ, was the same as that of YSZ. Doping of ZrO2 with alkaline earth metal cations (A^{2+}) is much less effective compared to rare earth dopants. This is due to a higher tendency to defect association and to a lower thermodynamic stability of the cubic fluorite-type solid solutions in ZrO_2–AO systems[21]. Some attempts have been made to search for new solid–electrolyte compositions in ternary systems. For example, the addition of calcium to YSZ can lead to a reduction in the activation energy for conduction[36]. Another approach to improving mechanical properties of zirconia solid electrolytes has been to add small amounts of highly dispersed alumina but at the same time, has been shown to both increase[37–39] and decrease[37,40] the conductivity of YSZ, depending on the doping level. S. Sarat et al.[41] have studied the effect of Bi_2O_3 addition of on the structure and electrical properties of ScSZ, reporting a sharp increase in conductivity.

3.2. *Intermediate temperature electrolyte*

Significant efforts have been addressed to reduce the operating temperature of SOFCs using different electrolyte materials which show higher ionic conductivities at relatively low temperatures. Like zirconia, ceria forms the fluorite structure and is a common electrolyte material for SOFCs also for its good compatibility with electrodes[42–44].

Figure 4: Fluorite crystal structure of ceria-based electrolytes[3].

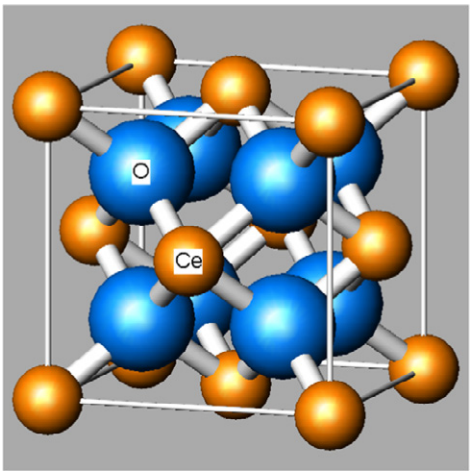

As compared to zirconia, ceria has a higher conductivity, particularly at low temperatures. Pure ceria is a mixed ionic electronic conductive material (MIEC)[45]. Despite its favourable ion transport properties, ceria had not, until quite recently, been considered a realistic candidate for fuel cell applications because of its high electronic conductivity. In particular, under reducing conditions, CeO2 (Fig. 4) is not stable and becomes CeO_{2-x}[35,42,46–49]. Now it is generally agreed that the main compensating defects in CeO_{2-x} are oxygen vacancies[35].

This has two main effects: first, it gives n-type electronic conductivity which causes a partial internal electronic short circuit in a cell, and second, it generates nonstoichiometry (with respect to normal valency in air) and expansion of the lattice which can lead to mechanical failure.

Overall, the ionic conductivity of ceria is approximately an order of magnitude greater than that of stabilized zirconia for comparable doping conditions. This is a result of the larger ionic radius of Ce^{4+} (0.87 Å in 6-fold coordination) than Zr^{4+} (0.72 Å), which produces a more open structure through which O= ions can easily migrate.

Equation 3.5 describes the ionic conductivity based upon the migration via oxygen vacancies.

$$\sigma T = \sigma_0 \exp\left(-\frac{\Delta E_{\text{act}}}{T}\right) \tag{3.5}$$

In this equation ΔE_{act}, the activation energy, involves both ΔH_m and ΔH_a, which are the enthalpy for migration of oxygen and the association enthalpy of defect complexes, respectively.

The electronic conductivity is caused by polaron hopping and can be described by equation (3.6), which has the Arrhenius form, as the electron mobility is temperature dependent.

$$\sigma_e T = \sigma_e^0 \exp\left(-\frac{\Delta H_n}{kT}\right) pO_2^{-\frac{1}{4}} \tag{3.6}$$

As becomes clear from these equations, while the ionic conduction is independent of the oxygen pressure, the electronic conductivity increases with increasing temperature and decreasing oxygen partial pressure. In addition, the electronic charge carriers are involved in the electrode process and the formation of the cell voltage. The electronic conductivity remains, however too low at high temperatures (about 0.16 S cm^{-1} at 800 °C). Although the strategy gives a transport number $t_0 \equiv \sigma_0/\sigma \approx 1$ in air or an inert atmosphere such as argon, Ce^{3+} ions are created in a reducing atmosphere to give a measurable electronic component σ_e in the total conductivity σ.

Like zirconia, ceria is doped to increase conductivity, and, also like zirconia, the highest conductivity occurs for ions with the lowest size mismatch. Doping the ceria with certain rare earth oxides of lower valences can markedly reduce the enthalpy of association. Balags and Glass[50] investigated ceria conductivity using 10 rare earth elements as dopants but the most used rare earth oxide generally are Gd_2O_3, Sm_2O_3 and Y_2O_3[51].

However, an increasing amount of dopants tends to form a second phase due to the solubility limit, resulting in the reducing of the conductivity. The lattice parameter of ceria doped with rare earth

oxides as a function of dopant concentration was measured by Bevan and Summerville[52], inferring that there is a linear relationship between the lattice parameter and the radius of dopant cations as confirmed by Yahiro et al.[51].

Among the three, gadolinium is the most common rare earth dopant, as ionic conductivity values have been shown to be nearly three times higher than the equivalent quantities of samarium doping[42]. The strong dependence of ionic conductivity on dopant type and concentration has been explained in terms of the lattice distortions introduced by the dopant, with those that produce the least amount of strain causing the smallest variation in the potential energy landscape. Reported open circuit potentials for doped ceria are lower than what one would expect on the basis of the electronic conductivity of ceria and represented simply as the multiple of the ionic transference number (greater than ~ 0.9[53] at 700 °C and 10^{-18} atm oxygen partial pressure) and the Nernst potential. For $Gd_{0.2}Ce_{0.8}O_2$ (GDC), which gives the highest oxide-ion conductivity of the rare-earth doped ceria,[54] the open circuit voltage of a hydrogen-air fuel cell was reduced to about 0.89 V at 650 °C[55].

Kudo et al.[56] and Yahiro et al.[57] measured the relationship between the conductivity of ceria with the level of doping with Gd_2O_3 and of Sm_2O_3 respectively. They found that the maximum conductivity was at around 20 mol%.

In 2003, our research group[58] has investigated the role of the preparation procedure on the electrochemical characteristics of CGO. We observed that powders of $Ce_{0.8}Gd_{0.2}O_2$ prepared by oxalic-coprecipitation and by acrylamide sol-gel routes were characterized by suitable bulk ionic. No electronic conductivity under air exposure and good electrochemical values were envisaged for both samples, though the acrylamide sol-gel process is preferable due to a small volume of reactants and large powder production with low costs.

Few experiments have been conducted in order to evaluate the electrical conductivities of ceria doped alkaline-earth oxides. Yahiro and co-workers[59] found that the electrical conductivities of ceria doped with MgO and BaO are exceptionally low, which may be ascribed to the insufficient solubility of these oxides in ceria.

In order to further increase conductivity and improve other related properties of the materials, co-doping approach have been extensively conducted and proved to be effective.

Probably, the most relevant research is that of Herle et al.[60] which found that co-doping ceria with alkaline earth and rare earth ion showed significantly higher conductivity in air than the best singly doped materials with the same oxygen concentration. Although, it is important to develop cost-effective ceria-based electrolyte materials with desired ionic conductivity for IT-SOFCs, many co-doped ceria have been investigated, such as $Ce_{1-x-y}Gd_xPr_yO_2$[61]; $Ce_{1-x-y}Sm_xLa_yO_2$[62]; $Ce_{1-x-y}Y_xLa_yO_2$[63], and $Ce_{1-x-y-z}Gd_xSm_yY_zO_2$[60].

The electronic leakage can be partially solved by a combination of doped ceria with other solid electrolytes such as stabilized zirconia or doped lanthanum gallate, in multilayer cells[48,49,64].

An additional challenge lies with the chemical expansion of ceria under reducing conditions and the internal stress that result[65]. At this stage, the significance of this issue on the long-term viability of ceria-based fuel cells is unknown. It is noteworthy that planar cells experience lower stresses than tubular cells, suggesting that clever designs may alleviate possible stresses.

Some novel oxygen ionic conductors have been recently reviewed, including perovskite-type oxides derived from lanthanum gallate $LaGaO_3$[29], doped bismuth oxide systems[34,66], and molybdate based materials with cubic structure ($La_2Mo_2O_9$)[67–69].

3.3. *Proton conductors*

In recent years, protonic conducting oxides have been widely studied due to their suitable protonic conductivity at intermediate temperatures. There are a number of materials which conduct protons, but most either decompose at temperatures above 300 °C or conduct only over 1000 °C[70]. A.K. Demin and P.E. Tsiakaras[71] have demonstrated that SOFC-H^+ shows higher thermodynamic efficiency for the conversion of chemical energy to electrical power rather than SOFC-O^{2-} for systems fed by hydrogen that in the range between 1000 and 1300 K exceeds 80%. In fact, when hydrogen is used as fuel, a proton conductor offers the benefits of generating water at the cathode, and thus the fuel does not become diluted during cell operation[72,73]. Ceramic proton conductors have a larger ionic transport number than ceria doped gadolinia and better chemical compatibility with conventional SOFC materials than lanthanum strontium gallates (LSGM). Furthermore, these oxides can work in the temperature range 400–750 °C in dependence of their lower activation enthalpies of their conductivity, and they represent a possible alternative to the classical SOFC electrolytes based on yttria stabilized zirconia which operates only at higher temperatures.

Ceramic proton conducting electrolytes thus compete with anionic CGO and LSGM for

application in intermediate temperature solid oxide fuel cells. However, the presence of protons in these materials has not structural protons. These materials derive their ionic conductivity from the incorporation of protonic defects which have sufficiently high mobility. D.G. Thomas and J.J. Lander[74] were the first to report the formation of proton defects at moderate temperature for the ZnO ascribed to the dissociative absorption of water during fabrication, characterization or use of oxide, which requires the presence of oxide ion vacancies.

The identified compounds are acceptor-doped perovskite-type oxides $AB_{1-x}M_xO_3$ (A = Ba, Sr; B = Ce, Zr, Ti) where A and B are the main constituents, M is a trivalent dopant, such as a rare earth element, and x is a dopant level less than 1. The basic perovskite-type structure, without a dopant, has the general form ABO_3 and an orthorhombic crystal structure. In this structure, component "A", the large metal cation, occupies the center of the crystal, "B", the small cation, occupies the corners, and oxygen, O, is in the center of the edges. When this basic structure is doped with a rare earth element such as yttrium (Y) or terbium (Tb), the dopant displaces some of the small cations ("B"). this substitution causes the formation of oxygen ion vacancies in the structure. In presence of an atmosphere that contains hydrogen and/or water at elevated temperatures, such materials often show significant proton conductivity. The conductivity is related to the protonic defects and the mobility is imputable to them concentration fall into a narrow range. Any symmetry reduction, however, leads to a drop of concentration and mobility of the protonic defects.

Stotz and Wagner[75] developed the present formalism of hydrogen in oxides: water from gas phase dissociates into a hydroxide ion and a proton; the hydroxide ion fills an oxide ion vacancy and, the proton forms a covalent bond with a lattice oxygen, that have a positive effective charge, and contribute to the conductivity. For a good protonic conductor this humidity-induced conductivity must be much larger than that of electronic defects (electrons or holes) or other ionic species such as oxygen ion vacancies. Standard protonic conducting oxides contain a high concentration of oxygen vacancies in the dry state which are partially filled in the humidifying conditions. In fact, due to the uniquely small ionic radius, protons can not occupy a lattice or normal interstitial site, but are always embedded in the electron cloud of an oxygen ion, forming a hydroxide defect. The migration of such light ions involves hopping mechanism. The transport properties in such model can be assisted lattice interaction and vibration[76] and the effect is that the protons show a low activation energy for the conduction (0.3–0.6 eV)[77–79].

In Kröger-Vink notation this reaction can be written:

$$H_2O + V_O^{\bullet\bullet} + O_O^x \Leftrightarrow 2(OH)_O^{\bullet}$$

where a water molecule is split into two hydroxide ions and they replace the oxide ions, i.e., two positively charged protonic defects are formed.

Among the best known and intensively investigated examples are alkaline earth cerates, zirconates, niobates and titanates. It is widely held that oxides with high conductivity (e.g. $BaCeO_3$-based compounds) generally show very low phase stability (e.g. with respect to carbonate of hydroxide formation[80].

The original materials investigated in this class were barium cerate ($BaCeO_3$) and strontium cerate ($SrCeO_3$). Empirical approaches to increase the stability of cerates by chemical modifications[81–83] seemed to confirm that high proton conductivity and stability are antagonistic properties[80].

In the early 1980s Iwahara et al.[84] have discovered that doping these materials with rare earth elements such as yttrium and terbium, greatly improves the protonic conduction. All the reported high temperature proton conducting ceramics are doped compounds, which can be largely classified into a number of categories based on the following oxides: (1) $SrCeO_3$, (2) $BaCeO_3$, (3) $SrZrO_3$, (4) $SrTiO_3$, (5) $BaSnO_3$, (6) complex perovskites in the forms of quaternary oxides such as $A_2B'B''O_6$ and $A_3B'B''O_9$. This latest class of perovskite are to be almost always referred as niobates and tantalates in which the "A" ions are always charged 2+, B′ and B″ ions have charges 3+ and 5+, respectively (e.g., Sr_2ScNbO_6), while in the second they are 2+ and 5+, respectively (e.g., $Sr_3CaNb2O_9$) with the mean B-ion valence 4+ and a cation charge deficit due to a relative stoichiometry between B' and B'' cations, which is compensated by oxygen vacancies or protons[85–88]. In 2002, Irvine and co-workers[89] have investigated $Sr_3CaZrTaO_{8.5}$ and related compositions which exhibited a protonic conductivity in wet 5% H_2/Ar of 4.6×10^{-4} S cm^{-1} at 300 °C with an activation energy of 0.66 eV[90] on a par with the structurally related proton solid electrolyte, $Ba_3Ca_{1.18}Nb_{1.82}O_{8.73}$ without loss of ordered perovskite lattice[91–93].

At the present, $SrZrO_3$ base materials have lower proton conductivity[94,95]; Indium (In) and Yttrium (Y) have been proposed as dopant of $BaSnO_3$ with doping rates as high as 50%[96,97] Émile Bévillon and co-workers have begun a systematic study of hydratation and proton conduction in barium

stannate from an experimental and theoretical point of view[98]; acceptor-doped $SrTiO_3$ has shown a less favourable formation of proton defects[99], whereas complex perovskite like as $Ba_3Ca_{1.24}Nb_{1.76}O_{9-\delta}$ has shown very low electronic conductivity[93].

However, none of these compounds concurrently satisfies two of the essential requirements for IT-SOFC application: high proton conductivity, good chemical stability under fuel cell operating environment. As well as a number of other parameters might be optimises: densification, thickness thermal expansion, mechanical stability and ionic transference number.

In 1997, Guan[100] studied the conductivity of bulk of 5% yttrium-doped $BaCeO_3$ (BCY) in the form of 2.2 cm diameter pellets. The group tested the material from 500 °C to 800 °C and in both oxygen/water vapor and hydrogen/water vapor atmospheres. They found that proton conduction is dominant at lower temperatures (500–600 °C) and oxygen ion conductivity is dominant at higher temperatures. Protonic conductivity ranged from 1.9×10^{-3} (S cm^{-1}) at 800 °C in oxygen/water vapor atmosphere to 1.27×10^{-2} (S cm^{-1}) at 800 °C in a hydrogen/water atmosphere. Total conductivity in a hydrogen/water atmosphere ranged from 4.37×10^{-3} (S cm^{-1}) at 600 °C to 1.99×10^{-2} (S cm^{-1}) at 800 °C.

In 2002, Hibino[101] constructed a solid oxide fuel using BCY as the electrolyte using the Pt as electrodes, conductivities for a 10% Y-doped $BaCeO_3$ electrolyte ranged from $\sim 1.9 \times 10^{-3}$ (S cm^{-1}) at 400 °C to $\sim 9 \times 10^{-3}$ at 600 °C in a H_2 saturated with H_2O atmosphere. Hibino found that BCY conductivity was higher than for YSZ for temperatures below about 650 °C, but that YSZ conductivity was higher than BCY for temperatures above 650 °C.

Activation energies were only reported for the 25% Y-doped composition, but these range from 0.41 eV (400–500 °C) to 0.53 eV (550–800 °C).

With $BaCeO_3$, the dopant element of choice has typically been yttrium, though other elements have been researched. Recently[102], our research group has investigated two protonic electrolytes such as $BaCe_{0.8}Y_{0.2}O_3$ and $BaCe_{0.9}Y_{0.1}O_3$. The cerate powders were ball-milled for 14 h, and then uniaxially pressed into pellets in a die under a pressure of 400 MPa. The green pellets were sintered at 1450 °C for 6 h in nitrogen atmosphere, to obtain dense substrates. In fact, the high basicity of these oxides is advantageous for the formation of protonic charge carriers but, on the other hand, basic oxides are expected to react easily with acidic or even amphoteric gases like SO_3, CO_2, H_2O to form the respectively sulfates, carbonates and hydroxides[80].

The density was larger than 95% of theoretical value. After the thermal treatment a color change was observed. In fact, the samples turned from white to black.

The same phenomenon is reported in the literature[103,104] for anionic electrolytes based on lanthanum gallate with a perovskite structure. However, from a careful analysis of their diffraction patterns this does not seem to be related to the presence of secondary phases. A slight formation of Ce^{3+} ions is not excluded[42]. Yet, this does not appear to affect the open circuit voltage of the SOFC cells equipped with these protonic electrolytes.

A good crystallographic and compositional purity, in the pellet of both cerates after the thermal treatment at 1450 °C, was observed from XRD diffractograms (Fig. 5). In fact, no evidence of crystallographic peaks associated with carbonates at about 24° 2θ, appeared after the high temperature treatment. In the pellet with the highest amount of Y (20 wt%) a shift of the diffraction peaks towards higher Bragg angles was observed; this indicates a lattice contraction. Recently, further analysis on $BaCe_{0.8}Y_{0.2}O_3$ has been proposed by I-Ming Hung and co-workers[105]. These authors observed that the symmetry of the protonic conductor became tetragonal as dopant effect for Y^{3+} amount up to 20 mol.

Besides, X-ray photoelectron spectroscopy (XPS) analyses, carried out on the surface of the pellets after the thermal treatment, revealed the presence of the peak at 289 eV in the C 1s that is attributed to a small amount of carbonate on the surface. This signal is significantly smaller in the $BaCe_{0.8}Y_{0.2}O_3$ vs. $BaCe_{0.9}Y_{0.1}O_3$ sample (Fig. 6).

Further analysis was carried out for the $BaCe_{0.8}Y_{0.2}O_3$ sample due to the better crystallographic purity. Arrhenius plot (Fig. 7) was obtained by interpolation of bulk conductivity values for the $BaCe_{0.8}Y_{0.2}O_3$ electrolyte recorded in a wet hydrogen atmosphere with relative humidity (R.H.) of 3%, at 100 °C intervals (except for the first point obtained at 150 °C) whereas the conductivity values of $Ce_{0.8}Gd_{0.2}O_{1.95}$ (CGO) electrolytes as comparison were reported in our previous study [58]. The $BaCe_{0.8}Y_{0.2}O_3$ electrolyte has a conductivity of 3.2 9 10^{-3} S cm^{-1} at 700 °C. This value is lower than the corresponding one obtained for an anionic electrolyte such as $Ce_{0.8}Gd_{0.2}O_{1.95}$[106–109]. The conductivity of the protonic electrolyte is smaller than that reported in the literature[110]. This may be in part related to the different R.H. values adopted for the measurements.

Possibly, the conductivities of the barium cerate-based materials could be further increased by complete elimination of the small traces of the

Figure 5: XRD patterns of $BaCe_{0.9}Y_{0.1}O_3$ and $BaCe_{0.8}Y_{0.2}O_3$ after the thermal treatment in nitrogen atmosphere at 1450 °C for 6 h. The insert shows the shift of the cerates main signal indexed (002) [Ref. 102].

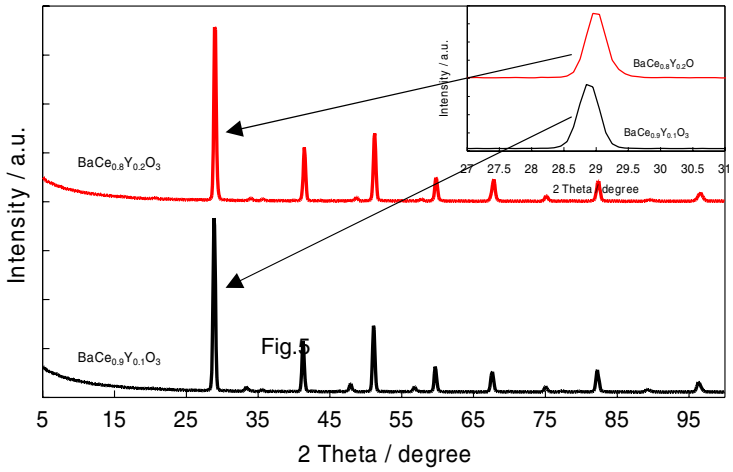

Figure 6: XPS spectrum of the BaCe0.9Gd0.1O3 (a) BaCe0.8Gd0.2O3 (b) after the thermal treatment in nitrogen atmosphere at 1450 °C for 6 h [Ref. 102].

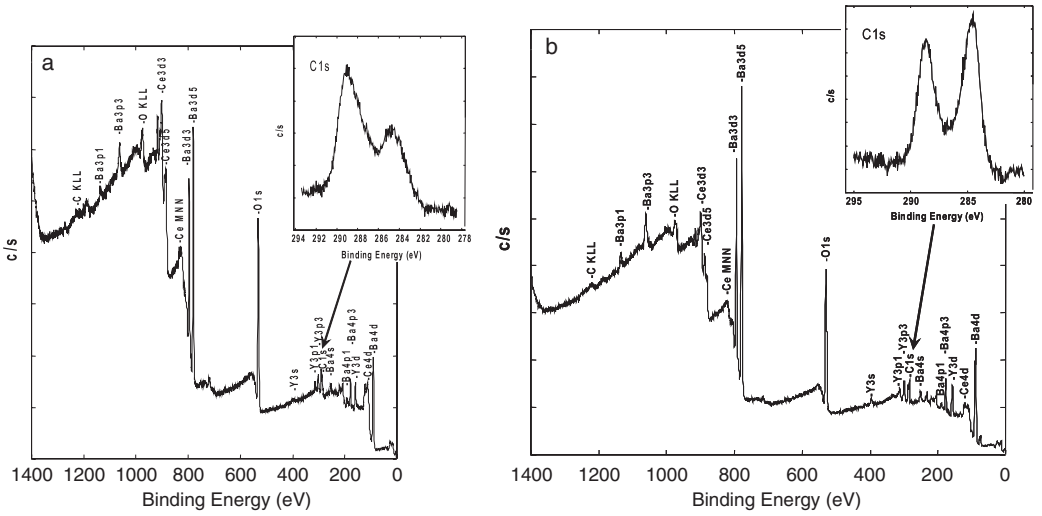

insulating $BaCeO_3$ phase. The activation energy for $BaCe_{0.8}Y_{0.2}O_3$ obtained from the slope of the Arrhenius plot is 0.4 eV; this is in agreement with the literature[111]. Moreover, this value is considerably lower than those observed for the anionic electrolytes (0.8 eV)[32]; this indicates a lower activation with temperature and, consequently, the possibility to operate at low temperatures.

Moreover, in order to estimate the ionic transport number the protonic electrolytes properties were investigated at 600 °C in a SOFC device fed with a mixture of Ar/H_2 (3% H_2O) at the anode and static air at the cathode. Silver electrodes at both faces of the pellet were used in these experiments. The open circuit voltage values were measured at different H_2 concentrations in the range 0–100% after appropriate conditioning and compared to those obtained with CGO electrolytes in the presence of silver electrodes and at the same temperature as well.

Figure 7: Arrhenius plot of bulk conductivity of BCY (20% Y) and of CGO (20% Gd) in a wet hydrogen atmosphere with relative humidity (R.H.) of 3% [Ref. 102].

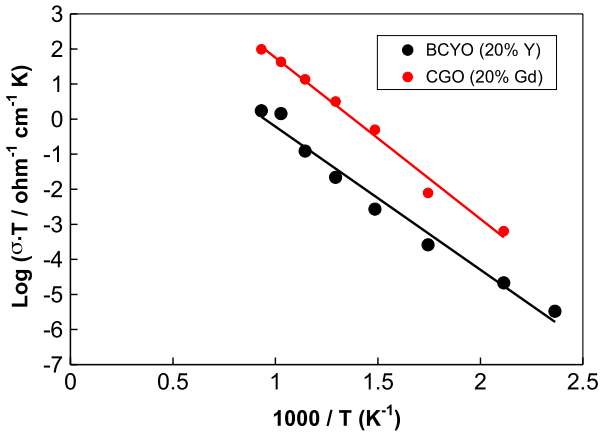

Figure 8: Open circuit potential as a function of H_2 concentrations for protonic electrolyte based cell ($BaCe_{0.8}Y_{0.2}O_3$) at a temperature of 600 °C and relative humidity (R.H.) of 3% [Ref. 102].

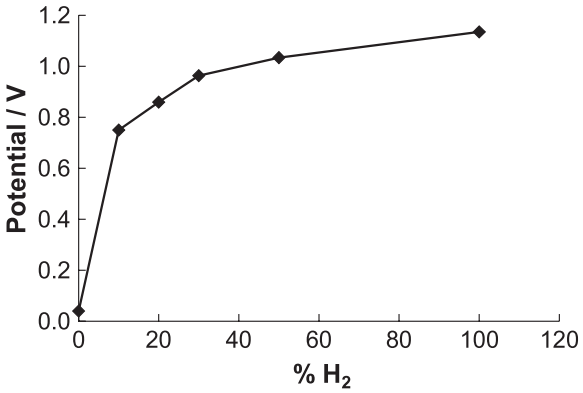

As shown in Fig. 8, upon increasing the H_2 concentration, the OCV increases from a value of about 50 mV to a value of 1.14 V. This latter is comparable to the thermodynamic value for 100% H_2/air. Thus, it seems that the ionic transport number is roughly unity. This is not the case for CGO where, under the same conditions, an OCV value of 0.85 V was achieved[112], which would correspond to an ionic transport number of about 0.8. Thus, a significant fraction of energy is lost at low current densities owing to a parasitic electron transport through the electrolyte ($Ce^{4+} \leftrightarrow Ce^{3+}$ process). As envisaged by Steele[42], this effect for CGO is less significant at high currents due to the presence of weaker reducing conditions.

Finally, two cells with the same electrodes but with a different electrolyte were electrochemically characterized. The thickness of the electrolyte was 300 μm in both cases. The results were compared in order to evaluate the differences in performance between a protonic electrolyte based-cell and an anionic cell with same electrodes and architecture.

Ac impedance spectra[113] of the BCY ($BaCe_{0.8}Y_{0.2}O_3$) supported cell operating in the presence of H_2 in the range 700–800 °C are shown in Fig. 9. The series resistance (Rs) derived from the high frequency intercept on the real axis of the Nyquist plot decreases from 2.1 Ω cm^2 at 700 °C to 1.38 Ω cm^2 at 800 °C.

Ac impedance spectra of the CGO supported cell are shown in Fig. 10. The series resistance decreases from 0.34 Ω cm^2 at 700 °C to 0.21 Ω cm^2 at 800 °C. It appears that the series resistance of the cell based on the CGO electrolyte is significantly

Figure 9: Nyquist plots at open circuit voltage (OCV) as a function of the temperature obtained for a protonic electrolyte (BCY) supported cell fed with H_2 [Ref. 102].

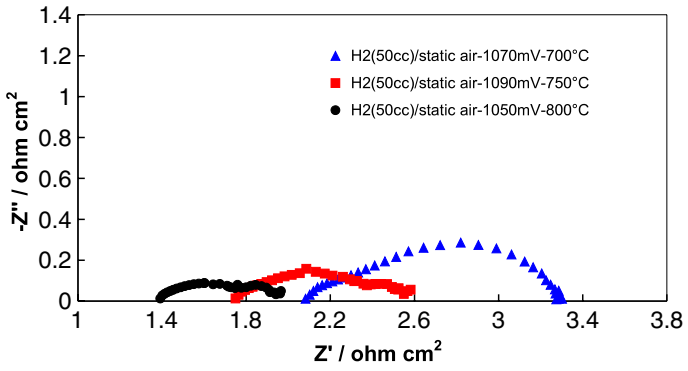

Figure 10: Nyquist plots at open circuit voltage (OCV) as a function of the temperature obtained for an anionic electrolyte (CGO) supported cell fed with H_2 [Ref. 102].

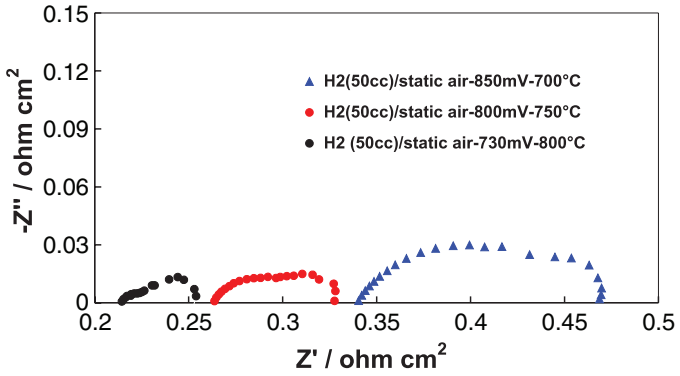

smaller than that of the cell equipped with the protonic electrolyte at all temperatures.

This effect is mainly due to the better ionic conductivity of CGO compared to BCY. The charge transfer resistance (RCT) was obtained by the difference between the low and high frequency intercept on the Nyquist plot. RCT is often associated with activation polarization for low overpotential. The RCT is quite similar for CGO and BCY electrolyte based cells at 700 °C, but is significantly smaller (one half) for the CGO cell at 800 °C. The ac-impedance profiles consist of two main semicircles for both systems but, the profiles are quite different for the two cells at 700 °C. In the BCY cell, the semicircle at low frequency, mainly related to the cathode contribution, shows large impedance values, whereas, in the CGO based cell the semicircle at high frequency that is related to the anode prevails in terms of impedance. In this latter system the reduction of Ce^{4+} to Ce^{3+} plays a significant role, causing a parasitic current through the electrolyte. The different ac-impedance profiles indicate a significant role of the electrode-electrolyte interface.

As the performance of the BCY cell is strongly affected by the ohmic resistance of the electrolyte, in order to obtain a reliable comparison between the two cells in terms of interface characteristics, the IR-free polarization curves were calculated from raw polarization data. In Figs. 11 and 12 the IR-free polarization curves related to the BCY and CGO cells are shown. The maximum power densities obtained at 700 °C were 183 mW cm^{-2} for the BCY based-cell and 400 mW cm^{-2} for the CGO cell. The performances obtained for the anionic electrolyte supported cell are about twice higher than the protonic one. As stated by Steele[42] the effect of parasitic electron drag is significant for

Figure 11: V-I curves (IR-free) collected in the range 700–800 °C in H_2 for the cell based on a supporting protonic electrolyte (BCY) [Ref. 102].

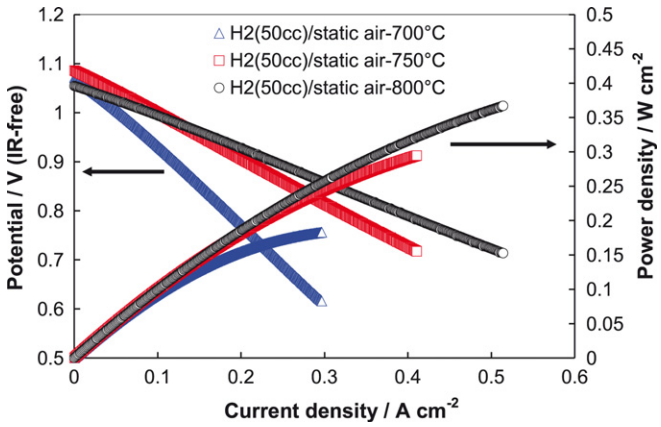

Figure 12: V-I curves (IR-free) collected in the range 700–800 °C in H_2 for the cell based on a supporting anionic electrolyte (CGO) [Ref. 102].

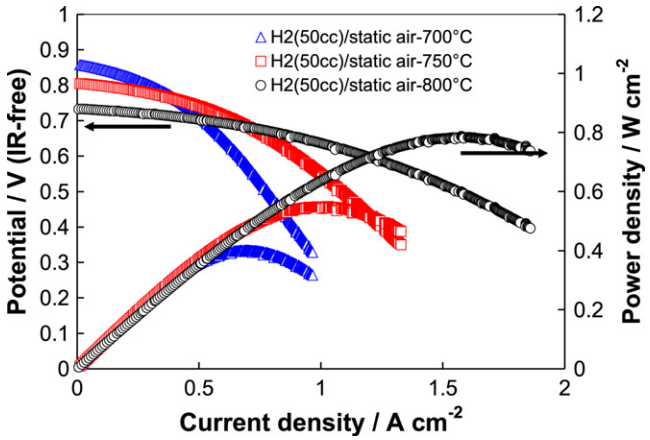

CGO electrolytes at conditions close to the OCV. At low current densities the BCY cell performs better than the CGO cell due to the higher ionic transport number. However, the low current density zone is not of practical interest. At reasonable current densities and cell voltages e.g. 0.7 V the CGO cell performs better than the BCY cell even at 700 °C. Due to its lower activation energy, it is likely that, at temperatures below 700 °C e.g. in the range 400–600 °C, the protonic may outperform the anionic electrolyte cell. However, at present, the performance recorded at such low temperatures does not appear to be of practical interest.

Chemical stability especially in CO_2 could be effectively improved by partial substitution of Zr for Ce as reported by many researchers[114–117]. It has been reported that 0.4 mol Zr substitution was enough to obtain good chemical stability[118]. However, the introduction of Zr reduced the electrical conductivity; on the other hand, it made the densification process more difficult. The typical sintering temperature was above 1550 °C to achieve desired relative density[115,118,119], which preclude the fabrication of co-sintered SOFC structures and the consequent mechanical stress. Besides, a long period of sintering at high temperatures easily resulted in Ba loss from A-site, which may degrade the properties of materials. Thus, developing an easier sintering process was desirable. Thus, developing an easier sintering process was desirable.

In 2009, Cuijuan Zhang et al. have studied the effect of the addiction of ZnO in different amounts as sintering aid for $BaZr_{0.85}Y_{0.15}O_3$[120].

T. Shimada and co-workers[121] have focused them attention on a practical protonic conductor of $BaZr_{0.4}Ce_{0.4}In_{0.2}O_3$ that has a relatively high durability against moisture and good protonic conductivity. From the results of concentration cell measurements, it was revealed that this proton conductor has good proton conductivities in hydrogen-rich atmospheres and behaves as a protonic and oxide ionic conductor in oxygen-rich atmospheres, with some extent of electronic conductivity, which lowers its ionic transport number.

Still Guan et al. in the 1998 have led the investigation of proton-conduction in other perovskite oxide, showing that Yttrium doped strontium cerate tends to have slightly lower proton conductivity then yttrium doped barium cerate, but it also exhibits less oxygen-ion conductivity and is generally more stable[122].

Terbium (Tb)[123,124], thulium (Tm)[125], and ytterbium (Yb)[126], have been proposed as dopants for $SrCeO_3$, because can have a dramatic effect on the properties of the film. X. Qi and Y.S. Lin[123,124] have reported that the conductivity of both terbium and thulium doped strontium cerates obey the Arrhenius relationship in atmospheres of O_2, air, and N_2. The presence of water vapor lowers both the conductivity values and the activation energies in oxidative atmospheres, suggesting a mixed proton–electron conducting property of the thulium doped $SrCeO_3$ whereas even if the humidity affects the electrical conductivity in nitrogen, air or oxygen rather than in hydrogen or methane, terbium doped $SrCeO_3$ is a pure protonic conductor with very low electronic and oxygen ionic conductivity.

In 1999[127], a fundamental study about interatomic distances by means of extended X-ray absorption fine structure (EXAFS) in proton conductive $SrCe_{1-x}Yb_xO_3$ has shown that though the difference in the electronegativity and ionic radius between Ce and Yb is small, in contrast to the case of Yb-doped $SrZrO_3$, the oxygen vacancies are distributed homogeneously around Yb and Ce rather than preferential localization around dopant Yb, supporting the higher protonic conductivity of doped $SrZrO_3$.

Actually, being the electronic conductivity of terbium doped perovskite several orders of magnitude lower than that of yttrium doped $SrCeO_3$, it is preferable rather than $SrCe_{1-x}Y_xO_3$.

Recently, an even better correlation has been found between the hydration enthalpies and the differences of the electronegativities of A and B site cations[128], i.e., the most negative hydration enthalpies have been reported for similar electronegativities of A and B site cations. Whether this is indicative of any particular physico-chemical concept is not clear, because data only for perovskites with Sr and Ba (i.e., A site elements with similar electronegativities) have been compared. The variation of the electronegativity for the B site element is much larger, and there is a clear trend for the equilibrium constant of the hydration reaction, which decreases in the order cerate → zirconate → stannate → niobate → titanate, i.e., with increasing electronegativity of the B site cation[99].

According to the present research, strontium cerates has been somewhat eclipsed due to mechanical deficiencies and its CO_2 sensitivity. Barium cerates are widely investigated group of compounds has fewer of the above problems and also a higher protonic conductivity. Alkaline earth zirconates are chemically and mechanically more stable than cerates or titanates ceramics but lower protonic conductivity. Complex perovskites which are considered the rather new compounds with rather good protonic conductivity at low temperatures, apparently become promising.

3.4. *Mixed ions conductors for low temperature SOFCs*

Until recently, SOFCs were limited to the IT-SOFC operating temperature range due to a lack of electrolyte systems that could exhibit the required conductivities needed to provide acceptable power outputs. It was found that combining the traditional cationic doped ceria, e.g. gadolinium doped ceria (GDC), yttrium doped ceria (YDC), and samaria doped ceria (SDC) with various salts, e.g. chlorides, fluoride, nitrate, and hydroxides[129,130], as well as soon afterwards, more traditional SOFC elements such as alumina, other kind of rare-earth oxides based on the ceria, and carbonates settled on as the salt material[131]. These materials contain at least two phases and are commonly referred as proton conducting salts and salt-oxide composites (SOCs), e.g. the ceria phase and the salt phase, or by two rare-earth oxides based on the ceria, which produce a large increase in the ionic conductivity of the electrolyte. These systems represent a relatively new research field that could be promising for low temperature solid oxide fuel cell (LT-SOFC) application and in particular this latest class offers a combination of high conductivity and performance while abstaining from using the highly corrosive salts popular in the late 90s.

This conductivity enhancement was often explained by pioneering researchers as an ionic transport system which has at least one molten

(liquid)-like state for the mobile ion species within a rigid lattice framework. At operation temperature, the salt can be molten with very high ion mobility and the solid oxide provides the rigid lattice framework of the system up to high temperatures. An ideal system is constituted by small amount of salt highly distributed in the solid matrix and incorporated in the interfacial regions of the oxide grains. The final result would be a system remaining as a solid-like state with enhanced interfacial pathway conductivity due to a composite effect, but at the same time, not weakened in the mechanical strength. Traditional theory would suggest that ion conductivity is exclusively imputable to the solid oxide phase through the diffusion of oxygen defects whereas molten salt conduces protons. It is beyond all that the faster ion conduction is dominated by interfacial phenomena. The most reliable conduction mechanism is that discovered by Førland and Krogh-Moe in 1957[132], successively described by Lunden[133] and depicted as the "paddle wheel" aid. In this model, the proton embedded in the electronic cloud of one host ion travels to another. The migration is assisted and enhanced by the rotation or oscillation motions of the interfacial salt sites, where H+ is coupled, providing a conduction pathway.

4. Summary

Mechanisms understanding is the key for developing new or better electrolytes for solid oxide fuel cells. Operation at low temperatures may overcome the present limitations. We have reviewed in this article the properties and perspectives of several alternative electrolytes varying in terms of chemistry, crystal structure and electrical properties. Concerning with the ion transport mechanisms, the electrolytes were classified in three different classes: anionic, protonic and mixed ions. Our recent research efforts on IT-SOFC systems have been outlined. A comparison between the most common electrolytes for intermediate temperature operation with different ion transport mechanisms, such as gadolinia doped ceria and yttrium doped barium cerate, have been reported.

Acknowledgement

We are indebted to our Director of the CNR-ITAE Institute, Dr. Gaetano Cacciola, for his continuous support of our activities and the careful review of the manuscript.

Received 29 September 2009; revised 18 December 2009.

References

1. M. Juhl, S. Primdahl, C. Manon, M. Mogensen, J. Power Sources 61, (1996), 173
2. Brown, M.; Primdahl, S.; Mogensen, M., J. Electrochem. Soc. 147, (2000), 475
3. J.A. Kilner, B.C.H. Steele, in: O.T. Sorensen (Ed.), Non-stoichiometric Oxides, Academic Press, New York, (1981), 233
4. N.Q. Minh, T. Takahashi, Science and Technology of Ceramic Fuel Cells, Elsevier, Amsterdam, The Netherlands, (1995), 69
5. R.T. DeHoff, Thermodynamics in Materials Science. McGraw-Hill Inc., New York, NY, (1993), 355
6. C.H.P. Lupis, Chemical Thermodynamics of Materials. Prentice Hall Publishing, New York, NY, (1993), 152
7. A.V. Virkar, J. Chen, C.W. Tanner and J.W. Kim, Solid State Ionics 131, (2000), 189
8. W. G. Coors, J. Power Sources 118, (2003), 150
9. W. Nernst, Z. Elektrochem. 6, (1899), 41
10. An Introduction to Materials Engineering. and Science for Chemical and Materials. Engineers. By Brian S. Mitchell, Wiley, Hoboken, NJ, (2004) 72
11. D.W. Strickler,W.G. Carlson, J. Am. Ceram. Soc., 47, (1964), 122
12. J.M. Dixon, L.D. LaGrange, U. Mergen, C.F. Miller, J.T. Porter, J. Electrochem. Soc., 110, (1963), 276.
13. X. Guo, J. Maier, J. Electrochem. Soc., 148, (2001), E121
14. T.-H.Yeh,W.-C. Hsu, C.C. Chou, J. Phys. IV France, 128, (2005), 213.
15. O. Yamamoto, Y. Arati, Y. Takeda, N. Imanishi, Y. Mizutani, M. Kawai, Y. Nakamura, Solid State Ionics, 124, (1995), 137
16. H.A. Johansen, J.G. Cleary, J. Electrochem. Soc., 111, (1964), 100
17. D.K. Hohnke, J. Phys. Chem. Solids, 41, (1980), 777
18. J.-H. Lee, S.M. Yoon, K.-K. Kim, J. Kim, H.-W. Lee, H.-S. Song, Solid State Ionics, 144, (2001), 175
19. I.Yu. Prokhorov, Electrochemical Society Proceedings, 2005-07, SOFC IX, (2005), 998
20. E. Djurado, F. Boulch, L. Dessemond, Electrochemical Society Proceedings, 2003-07, SOFC VII, (2003), 160
21. T.H. Etsell, S.N. Flengas, Chem. Rev., 70, (1970), 339
22. V.V. Kharton, E.N. Naumovich, A.A. Vecher, J. Solid State Electrochem., 3, (1999), 61
23. O. Yamamoto, Y. Arachi, H. Sakai, Y. Takeda, N. Imanishi, Y. Mizutani, M. Kawai, Y. Nakamura, Ionics, 4, (1998), 403
24. S.P.S. Badwal, Solid State Ionics, 52, (1992), 23
25. C. B. Choudhary, H. S. Maiti and E. C. Subbarao, in, Solid Electrolytes and their Applications, ed. E. C. Subbarao, Plenum Press, New York, (1980), 49
26. S.P.S. Badwal, F.T. Ciacchi, D. Milosevic, Solid. State Ionics, 136–137, (2000), 91
27. K. Nomura, Y. Mizutani, M. Kawai, Y. Nakamura, O. Yamamoto, Solid State Ionics, 132, (2000), 235
28. M. Hirano, S. Watanabe, E. Kato, Y. Mizutani, M. Kawai, Y.Nakamura, J. Am. Ceram. Soc., 82, (1999), 2861
29. V.V. Kharton, F.M.B. Marques, A. Atkinson, Solid State Ionics, 174, (2004), 135
30. J.W. Fergus, J. Mater. Sci., 38, (2003), 4259
31. R. Pornprasertsuk, P. Ramanarayanan, D.B. Musgrave, F.B. Prinz, J. Appl. Phys., 98, (2005) 1062513-1
32. H. Inaba, H. Tagawa, Solid State Ionics, 83, (1996), 1
33. H.J.M. Bouwmeester, A.J. Burggraaf, in: A. Burggraaf, L. Cot (Eds.), Fundamentals of Inorganic Membrane Science and Technology, Elsevier, Amsterdam, (1996), 435.
34. N.M. Sammes, G.A. Tompsett, H. Nafe, F. Aldinger, J. Eur. Ceram. Soc., 19, (1999), 1801
35. M. Mogensen, N.M. Sammes, G.A. Tompsett, Solid State Ionics, 129, (2000), 63
36. M.M. Bucko, Mater. Sci. Poland, 24, (2006), 39
37. M. Mori, T. Abe, H. Itoh, O. Yamamoto, Y. Takeda, T. Kawahara, Solid State Ionics, 74, (1994), 157
38. D. Lybye,Y.-L. Liu, M. Mogensen, S. Linderoth, Electrochemical Society Proceedings, 2005-07, SOFC IX, (2005), 954

39. N.H. Menzler, R. Hansch, R. Fleck, G. Blass, H.P. Buchkremer,H. Schichl, D. Stover, Electrochemical Society Proceedings, 2003-07, SOFC VII, (2003), 238
40. X. Guo, Phys. Stat. Sol. (a), 183, (2001), 261
41. S. Sarat, N. Sammes, A. Smirnova, J. Power Sources,160, (2006), 892
42. B.C.H. Steele, Solid State Ionics, 129, (2000), 95
43. S.W. Zha, C.R. Xia and G.Y. Meng, J. Power Sources, 115, (2003), 44.
44. S. Kuharuangrong, J. Power Sources, 171, (2007), 506
45. W.Z. Zhu, S.C.Deevi, Materials science & engineering A, 362, (2003), 228
46. M.V. Perfilyev, A.K. Demin, B.L. Kuzin, A.S. Lipilin, High-Temperature Electrolysis of Gases, Nauka, Moscow, (1988)
47. M. Goedickemeier, L.J. Gauckler, J. Electrochem. Soc., 145, (1998), 414
48. A. Atkinson, Solid State Ionics, 95, (1997), 249
49. I. Yasuda, M. Hishinuma, in: T.A. Ramanarayanan (Ed.), Ionic and Mixed Conducting Ceramics III, The Electrochemical Society, Pennington, NJ, (1998), 178
50. G.B. Balags and R.S. Glass, in: Proc. 2nd Intern Symp. on Ionic and Mixed Conducting Ceramics, eds. T.A. Ramanarayanan, W.L. Worrell and H.L. Tuller, The Electrochemical Society, (1994)
51. H. Yahiro, K. Eguchi and H. Arai, Solid State Ionics, 36, (1989), 71
52. D.J.M. Bevan and E. Summerville. In: K. A. Gschneidner, Jr. and L. Eyring, Editors, Handbook on the Physics and Chemistry of Rare Earths 3, North-Holland, Amsterdam (1979).
53. C. Miliken, S. Guruswamy, A. Khandar, J. Am. Ceram. Soc., 85, (2002), 2479
54. K. Eguchi, T. Setoguchi, T. Inoue, and H. Arai, Solid State Ionics, 52, (1992), 165
55. C. Lu, W. L. Worrell, R. J. Gorte, and J. M. Vohs, Journal of the Electrochemical Society, 150, (2003), A354
56. T. Kudo and H. Obayashi. J. Electrochem. Soc., 123, (1976), 415
57. H. Yahiro, Y. Eguchi, K. Eguchi and H. Arai. J. Appl. Electrochem., 18, (1988), 527
58. A. Sin, E. Kopnin, Y. Dubitsky, A. Zaopo, A.S. Aricó, L.R. Gullo, D. La Rosa, S. Siracusano, V. Antonucci, C. Oliva, O.Ballabio, Solid State Ionics, 175, (2004), 361
59. H. Yahiro, T. Ohuchi, K. Eguchi and H. Arai, J. Mater. Sci., 23, (1988), 1036
60. J.V. Herle, D. Seneviratne and A.J. McEvoy, J. Eur. Ceram. Soc., 19,(1999), 837
61. S. Lubke, H.-D. Wiemhofer, Solid State Ionics,117, (1999), 229
62. T. Mori, J. Drennan, J.-H. Lee, J.-G. Li, T. Ikegami, Solid State Ionics, 154–155, (2002), 461
63. H. Yoshida, H. Deguchi, K. Miura, M. Horiuchi, Solid State Ionics, 140, (2001), 191
64. A. Tsoda, A. Gupta, A. Naoumoidis, D. Skarmoutsos and P. Nikolopoulos, Ionics, 4, (1998), 234
65. A. Atkinson and T. M. G. M. Ramos, Solid State Ionics, 129, (2000), 259
66. A.M.Azad, S.Larose and S.A.Akbar, Journal of Materials Science, 29, (1994), 4135
67. Q. Fang, X. Wang, Z. Cheng, G. Zhang, Front. Mater. Sci. China, 1, (2007), 7
68. P. Lacorre, F. Goutenoire, O. Bohnke, R. Retoux, Y. Laligant, Nature, 404, (2000), 856
69. J.B. Goodenough, Nature, 404, (2000), 821
70. H. Iwahara. Solid State Ionics 77, (1995), 289
71. A. Demin and P. Tsiakaras, International Journal of Hydrogen Energy 26, (2001), 1103
72. S.M. Haile, Acta Materialia, 51, (2003), 5981
73. H. Iwahara, Y. Asakura, K. Katahira, M. Tanaka, Solid State Ionics, 168, (2004), 299
74. D.G. Thomas and J.J. Lander , J. Chem. Phys. 25, (1956), 1136
75. S. Stotz and C. Wagner, Ber. Bunsenges. Phys. Chem., 70, (1966), 781
76. A. L. Samgin, Solid State Ionics, 136-137, (2000), 291
77. E. Boehm, A.J. McEvoy, Fuel Cells, 1, (2006), 54.
78. H. Iwahara, T. Yajima, T. Hibino, H. Ushida, J. Electrochem. Soc., 140, (1993), 1687
79. N. Maffei, L. Pelletier, A. McFarlan, J. Power Sources, 136, (2004), 24
80. K. D. Kreuer, Solid State Ionics 97, (1997), 1
81. S. Wienströer and H.D. Wiemhöfer, Solid State Ionics 101–103 (1997), 1113
82. K. H. Ryu and S. M. Haile, Solid State Ionics, 125, (1999), 355
83. K. Katahira, Y. Kohchi, T. Shimura, H. Iwahara, Solid State Ionics, 138, (2000),91
84. H. Iwahara, T. Esaka, H. Uchida and N. Maeda, Solid State Ionics, 3–4, (1981), 359
85. A. S. Nowick and Y. Du, Solid State Ionics 77, (1995), 137
86. F.S. Galasso, Pergamon Press, New York, (1969)
87. F.S. Galasso, Gordon and Breach, New York, (1990), 15
88. I. E. Animitsa, Russian Journal of Electrochemistry, 45, (2009), 668
89. J.T.S. Irvine, Derek J.D. Corcoran, Anna Lashtabeg, John C. Walton Solid State Ionics 154–155, (2002), 447
90. D.J.D. Corcoran and J.T.S. Irvine, Solid State Ionics, 145, (2001), 307
91. K.C. Liang, Y. Du, A.S. Nowick, Solid State Ion. 69, (1994), 117
92. Y. Du, A.S. Nowick, Mater. Res. Soc. Symp., 369, (1995), 289
93. Y. Du, A.S. Nowick, J. Am. Ceram. Soc., 78, (1995), 3033
94. T.Yajima, H. Suzuki, T.Yogo, H. Iwahara, Solid State Ionics, 51, (1992), 101
95. T. Hibino, K. Mizutani, T. Yajima, H. Iwahara, Solid State Ionics, 58, (1992), 85
96. T. Schober, Solid State Ionics, 109, (1998), 1
97. P. Murugaraj, K.D. Kreuer, T. He, T. Schober and J. Maier, Solid State Ionics, 98, (1997), 1
98. É. Bévillon, G. Geneste, A. Chesnaud, Y. Wang, G. Dezanneau, Ionics, 14, (2008), 293
99. K.D. Kreuer, Solid State Ionics, 125, (1999), 285
100. J. Guan, S. E. Dorris, U. Balachandran, and M. Liu, Solid State Ionics, 100, (1997), 45
101. T. Hibino, A. Hashimoto, M. Suzuki, M. Sano, Journal of the Electrochemical Society, 149, (2002), A1503
102. D. La Rosa, M. Lo Faro, G. Monforte, V. Antonucci, A.S. Aricó, J. Appl. Electrochem 39, (2009), 477
103. B. Rambabu, S. Ghosh, W. Zhao, H. Jena, J Power Sources 159, (2006), 21
104. E. Djurado and M. Labeau, J. Eur. Ceram. Soc. 18 (1998), 1397
105. I.M. Hung., H.W. Peng, S.L. Zheng, C.P. Lin, J.S. Wu, Journal of Power Sources, 193, (2009), 155
106. Z. Tianshu, P. Hing, H. Huang, J. Kilner, Solid State Ionics, 148, (2002), 567
107. G.M. Christie, F.P.F. Van Berkel, Solid State Ionics, 83, (1996), 17
108. R.S. Torrens and N.M. Sammes, Solid State Ionics, 111, (1998), 9
109. R. Doshi and J.D. Carter, J. Electrochem. Soc., 146, (1999), 1273
110. H. Iwahara, Solid State Ionics, 86–88, (1996), 9
111. G. Ma, T. Shimura, H. Iwahara, Solid State Ionics, 110, (1998), 103
112. D. Prez-Coll, D. Marrero-Lpez, J.C. Ruiz Morales, P. Nez, J.C.C. Abrantes and J.R. Frade, J. Power Sources 173 (2007), 291
113. Q.-A. Huang, R. Hui, B. Wang and J. Zhang, Electrochim. Acta, 52, (2007), 8144
114. C.D. Zuo, S.E. Dorris, U. Balachandran and M.L. Liu, Chem. Mater., 18, (2006), 4647

115. K.H Ryu and S.M. Haile, Solid State Ionics, 125, (1999), 355
116. Z. Zhong, Solid State Ionics 178, (2007), 213
117. A.K. Azad and J.T.S. Irvine, Solid State Ionics, 178, (2007), 635
118. J. Li, J. Luo, T.K. Chuang and R.A. Sanger, Electrochimica Acta, 53, (2008), 3701
119. S. Tao and J.T.S. Irvine, Adv. Mater., 18, (2006), 1581
120. C. Zhang, H. Zhao, N. Xu , X. Li, N. Chen, International Journal of Hydrogen Energy, 34, (2009), 2739
121. T. Shimada, C. Wenb, N. Taniguchi, J. Otomo, H. Takahashi, Journal of Power Sources, 131, (2004), 289
122. J. Guan, S.E. Dorris, U. Balachandran, M. Liu, Solid State Ionics, 110, (1998), 303
123. X. Qi and Y.S. Lin, Solid State Ionics 120, (1999), 85
124. D. Dionysiou, X. Qi, Y. S. Lin, G. Meng, and P. D. Peng, Journal of Membrane Science, 154, (1999), 143
125. X. Qi and Y.S. Lin Solid State Ionics, 130, (2000), 149
126. H. Matsumoto, S. Hamajima, T. Yajima, H. Iwahara, Journal of the Electrochemical Society, 148, (2001), D121
127. Y. Arita, S. Yamasaki, T. Matsui, T. Harami, K. Kobayashi, Solid State Ionics 121, (1999), 225
128. T. Norby, Presented at Solid State Ionics Proc. SSPC-11, (2003) Surrey, England
129. B. Zhu, Solid State Ionics, 125, (1999), 397
130. B. Zhu, I. Albinsson, B. Mellander, and G. Meng, Solid State Ionics, 125, (1999), 439
131. B. Zhu, X. Liu, P. Zhou, X. Yang, Z. Zhu, and W. Zhu, Fuel Cells Bulletin, 5, (2002), 8
132. T. Førland and J. Krogh-Moe, Acta Chemica Scandinavica 11, (1957), 565
133. A. Lundén in: B. Scrosati, A. Magistris, C.M. Mari and G. Mariotto, Editors, Fast Ion Transport in Solids NATO ASI Series E:250, Kluwer, Dordrecht (1993), 181

Massimiliano Lo Faro Massimiliano Lo Faro was born in 1977. He graduated in Industrial Chemistry in 2002, and earned a PhD in Material Sciences at the University of Rome in 2008. Since 2003 he has worked at the Institute of Advanced Technology for Energy of the Italian National Research Council (CNR-ITAE 'Nicola Giordano'). Author of about 20 papers on topics related to Fuel Cells, he has received two awards from Dokiya and one from National Scientific committee for a Short-Term Mobility at the University of Thessaly. He is ECS member, secretary in steering committee of Younger Group of the Italian Chemical Society and delegate in the European Young Chemists Network.

Daniela la Rosa was born in 1975. She graduated in Industrial Chemistry in 2000. Since 2001 she has worked at the Institute of Advanced Technology for Energy of the Italian National Research Council (CNR-ITAE 'Nicola Giordano'), especially in the frqamework of a contract with Pirelli labs. Author of about 20 papers and several patents on topics related to Fuel Cells and electroceramics.

Vincenzo Antonucci Actually Project leader Distributed Energy Systems of CNR, Dept Energy and Transportation and Research Manager of Hydrogen and Fuel Cell Project at CNR- ITAE, President of Commission CEI (italy IEC section) WG 105 Fuel Cells, energy expert (MIUR Ministery of Research Italy, DG Tren, IEA) Member SRA and IP Working Group HFC Platform, Member Italian HFC Platform and Leader Deployment Group, Member of Management for the definition of Energy Plan for Sicily Region, Authors of more of 250 papers in Hydrogen and FC sector, in the top list (first 10 rank 6) of the authors in the Thomson reference list in Fuel Cell field. Vice Chair of the Research Grouping in the JTI (European Commission) for the planning of the Hydrogen and Fuel Cell activities in of the 7 FP. Experience in production, storage, distribution of hydrogen, fuel cells systems for transportation and distributed energy systems.

Antonino Salvatore Arico' is SOFC/DMFC project leader at the CNR-ITAE Institute and head of the group 'Processes for Energy Conversion' of the Italian National Council of Research. He was involved in research programmes related to the development of low and high temperature fuel cells. He has published more than 130 articles on International Refereed Journals. In the top list of the authors of the ESI-Topics on Fuel Cells (Thomson, rank 5), he is also author of 5 international patents and about 150 communications to conferences (about 10 invited presentations and keynotes lectures). He has been project responsible for several contracts including European Community projects such as MOREPOWER 6th Framework Program addressed to the development of portable power sources and SP leader in an Integrated project (Autobrane FP6) involving fuel cells.